## SQUIDs

Since the development of the Superconducting QUantum Interference Device (SQUID) in the late 1960s and its commercial introduction in 1970, SQUID-based instruments have proved to be the most sensitive measurement devices not only for magnetization measurements but also for a number of other electrical measurements. Their device noise (well below 1 mK), frequency response to dc, and low drift permit electromagnetic measurements at levels far below those of conventional techniques.

SQUID instruments consist of a SQUID amplifier or sensor and a detection circuit that transforms the signal of inter-

est into a magnetic flux that is detected by the SQUID sensor. Associated control electronics transform this signal into a room temperature voltage that is available for additional signal processing if needed. The SQUID amplifier and the detection coils are superconducting devices. Thus some type of refrigerant (e.g., liquid helium or nitrogen) or refrigeration device is needed to maintain the SQUID (and detection coil) in the superconducting state. Additional signal-conditioning electronics may be needed to improve the signal-to-noise ratio.

## THE JOSEPHSON EFFECT

SQUIDs combine two phenomena—flux quantization where the flux $\phi = \boldsymbol{B} \cdot \boldsymbol{A}$ penetrating a superconducting loop is quantized in steps of 1 $\phi_0 = h/2e = 2.068 \times 10^{-15}$ Wb, and the Josephson effect (1) (electrons tunneling from one superconducting region to another separated by a resistive barrier). Currents smaller than a critical current $I_C$, can penetrate the barrier (usually called a weak link) with no voltage drop (Fig. 1).

A typical weak link might have a critical current of 10 $\mu$A. If the loop has a diameter of 2 mm, this is equivalent to several flux quanta. In a superconductor loop interrupted by a weak link Josephson junction, magnetic flux threading through a superconducting loop sets up a current in the loop. As long as the current is below the critical current, the complete loop behaves as if it were superconducting. Any changes in the magnetic flux threading through the loop induce a shielding current that generates a small magnetic field to oppose the change in magnetic flux. The weak link can be a region in which the current flowing is greater than the current needed to drive the superconductor normal $I_C$. Details on the Josephson effect and the theory of SQUIDs can be found in References 2, 3, and 4.

## SQUID OPERATION

SQUIDs are operated as either RF (radio frequency) or dc SQUIDs. The prefix RF or dc refers to whether the Josephson junction(s) is biased with an alternating current (RF) or a dc current.

### The RF SQUID

For the RF SQUID (5), flux is normally (inductively) coupled into a SQUID loop containing a single Josephson junction via an input coil (which connects the SQUID to the experiment) and an RF coil that is part of a high-$Q$ resonant circuit to read out current changes due to induced flux in the SQUID loop (Fig. 2).

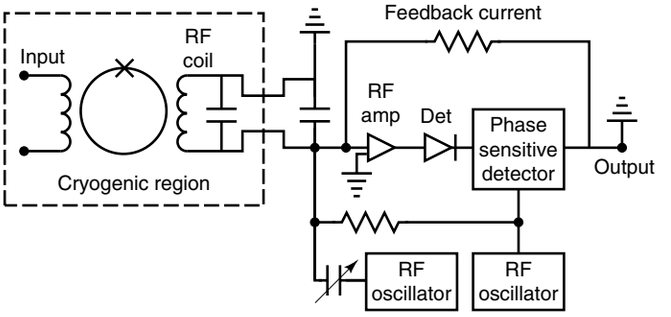


**Figure 2.** Block diagram of SQUID input and electronics for locked-loop operation.

This tuned circuit is driven by a constant current RF oscillator that is weakly coupled to the SQUID loop. The detected RF output is found to be the periodic function (Fig. 3).

One way to measure the change in input coil current is to simply count the number of periods it produces in the detected RF output. A more commonly used mode of operation is a feedback scheme (Fig. 2), which locks in on either a peak or a valley in the triangle pattern output from the RF peak detector. A feedback flux is applied to the SQUID through the RF coil that just cancels the change in flux from the input coil.

### The dc SQUID

The dc SQUID (Fig. 4) differs from the RF SQUID in the manner of biasing the Josephson junction (dc rather than ac) and the number of junctions (two rather than one).

The dc SQUID is biased with a dc current approximately equal to twice $I_C$ and develops a dc voltage across the junctions. A change in the flux penetrating the SQUID loop enhances the current through one Josephson junction and reduces the current through the other, driving one junction normally and the other superconducting. This asymmetry, which is periodic in $\phi_0$, is used to provide a feedback current that nulls the flux penetrating the SQUID loop. Although total flux within the SQUID loop is in multiples of $\phi_0$, by measuring the voltage drop across the feedback resistor, resolutions of external flux changes at the $10^{-6}$ level can be achieved. The linearity of flux-locked loop SQUID systems are

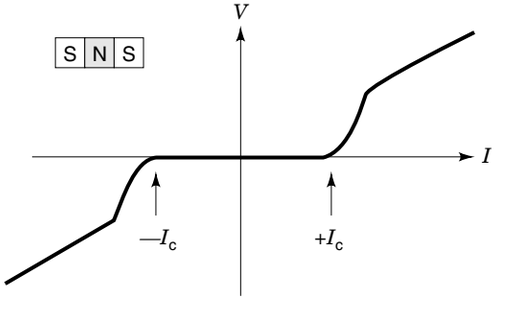


**Figure 1.** *IV* curve of a Josephson tunnel junction.

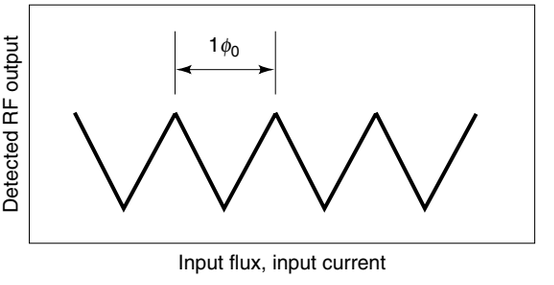


**Figure 3.** Triangle pattern showing detected output voltage as a function of flux in the SQUID.

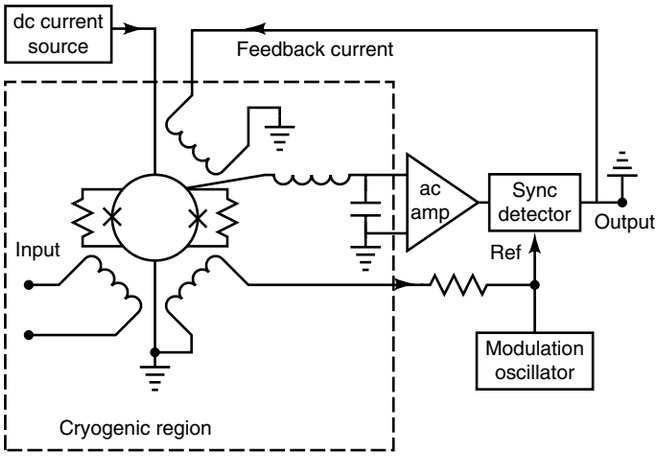


**Figure 4.** Block diagram of a typical dc SQUID.

typically better than 1 ppm. Like the RF SQUID, this feedback current (presented as a voltage at the output) is a direct measure of changes in flux applied to the SQUID.

**Control Electronics.** The system output voltage is the voltage drop across the feedback resistor in a negative feedback loop controlled by the SQUID electronics. The feedback signal is generated in response to changes in the output signal of the SQUID sensor. The output of the SQUID sensor is periodic in the field coupled into the SQUID loop. Negative feedback (similar to a phase-locked loop technique) is used to maintain the system operating point at a particular (and arbitrary) flux quantum. When operated in this mode, the system is in a flux-locked loop.

One important factor of SQUID design is such that the feedback electronics be able to follow changes in the shielding currents. If the shielding current changes so fast that the flux in the SQUID loop changes by more than $\phi_0/2$, it is possible that the feedback electronics will lag behind the rapidly changing flux. When the electronics finally "catch up," they can lock on an operating point (Fig. 3) different from the original. In this case, the SQUID has "lost lock" because the SQUID has exceeded the maximum slew rate of the electronics. This places an upper limit on the bandwidth of the system. The typical bandwidth of commercially available SQUID systems is dc to 50+ kHz. Custom electronics have been built extending bandwidths above 5 MHz. Typical slew rates for SQUIDs are in the range of $10^5$–$10^6$ $\phi_0$/s.

Even though one may not need or want to observe rapidly changing signals, situations may arise when ambient noise (e.g., 60 Hz) may determine the slew rate requirements of the system. To recover a signal from such interference, the system must be able to track all signals present at the input, including the noise. When system response is sped up to handle very fast signals, sensitivity to RF interference and spurious transients is also increased. Because the ability to remain locked while subjected to strong electrical transients is greatest when the maximum slew rate is limited (slow), whereas ability to track rapidly varying signals is greatest when the maximum slew rate is greatest (fast), it is desirable to be able to match the maximum slew-rate capability to the measuring situation. As a matter of convenience, many commercial SQUID systems offer user selectable slew rates along with high-pass and low-pass filters for noise reduction.

### Sensitivity

Because of the varying input impedances of SQUID sensors, the sensitivity of SQUID devices is best discussed in terms of the energy sensitivity:

$$E_N = L_i I_N^2 = \frac{\phi_N^2}{L_i} \tag{1}$$

where $L_i$ is the input inductance of the device, $I_N$ is the current noise, and $\phi_N$ is the flux sensitivity. $E_N$ is often expressed in terms of Planck's constant $h = 6.6 \times 10^{-34}$ J/Hz.

The major limiting factor in the noise of a RF SQUID is the bias frequency $f_0$ used to excite the tank circuit and that RF SQUID noise is proportional to $1/\sqrt{f_0}$ (6). As $f_0$ increases, the complexity of the electronics also tends to increase.

The minimum noise energy for a dc SQUID is given by (7)

$$E_N = k_B T \sqrt{L_{loop} C} \tag{2}$$

where $k_B$ is Boltzmann's constant, $L_l$ is the inductance of the SQUID loop, and $C$ is the capacitance of the junction. Substituting appropriate numbers indicates that the minimum noise energy $E_N$ for a dc SQUID is on the order of $h/2$. Devices with sensitivities of $\sim h$ have been constructed. These extremely low noise levels are achieved by limiting dynamic range and avoiding feedback. The need for practical (useful) devices requires that feedback be used and that the SQUID have a reasonable dynamic range. Commercially available RF SQUIDs have noise levels of $10^{-29}$ J/Hz; commercial dc SQUIDs are typically $\sim 10^{-31}$ J/Hz.

In addition to the frequency independent (white) component of system noise, there exists a low-frequency contribution that increases as the frequency decreases. The onset of this $1/f$ noise can be dependent on the ambient magnetic field when the SQUID sensor is cooled. When cooled in the earth's magnetic field, the point at which the $1/f$ noise equals the white (frequency independent) noise is typically $\sim$1 Hz. Cooling the SQUID sensor in low ambient magnetic fields (less than 1 $\mu$T) may improve the $1/f$ performance by as much as an order of magnitude. A large contribution to this noise in some dc SQUIDs can arise from the presence of the dc current bias. By chopping the dc bias in combination with the conventional flux modulation techniques, it is possible to reduce this added $1/f$ noise. This ac bias reversal approach (8) separates the original signal waveform from the noise associated with the dc bias and can reduce $1/f$ noise at very low frequencies.

The major difference between RF and dc SQUIDs is that the dc SQUID offers lower noise. From a historical viewpoint, although the dc SQUID was the first type of SQUID magnetometer made, the early development was with RF SQUIDs because of the difficulty in fabricating two nearly identical Josephson junctions in a single device. With modern thin film fabrication techniques and improvements in control electronics design, the dc SQUID offers clear advantages over the RF SQUID for many applications.

### Limitations on SQUID Technology

It is important to bear in mind several fundamental limitations in designing SQUID-based mesurement systems and data reduction algorithms.

1. A fundamental limitation of SQUIDs is that they are sensitive to *relative* (field or current) changes only. This is a consequence of the fact that the output voltage of a SQUID is a periodic function (Fig. 3) of the flux penetrating the SQUID loop. The SQUID is "flux locked" on an arbitrary maximum (or minimum) on the $V - \Phi$ curve, and the SQUID output is sensitive to flux changes relative to this lock point.
2. A second limitation exists on the system bandwidth. Although the SQUID has an intrinsic bandwidth of several gigahertz, when operated with standard flux-locked loop electronics using ac flux modulation, the maximum bandwidth is typically 50 kHz to 100 kHz. Another limitation is the presence of $1/f$ noise. High Temperature Superconducting (HTS) SQUIDs [and early commercial Low Temperature Superconducting (LTS) dc SQUIDs] exhibit excess $1/f$ noise due to critical current fluctuations of the Josephson junctions. This noise can be reduced by reversing the dc bias voltage (ac bias). This limits the maximum bandwidths less than half the bias reversal frequency. If the bias reversal frequency is too high, noise can be induced due to voltage spikes in the transformer coupled preamplifier input circuit. Because of this, the maximum bandwidth of present day HTS SQUIDs is ~30 kHz. If megahertz bandwidths are required, the ac bias is not used; however, there will be excess noise below 1 kHz.
3. Finally, SQUID magnetometers are vector magnetometers. For a pure magnetometer operating in the earth's magnetic field, a 180° rotation will sweep out a total field change of ~100 $\mu$T. If the magnetometer has a sensitivity of 10 fT/$\sqrt{\text{Hz}}$, tracking the total field change requires a dynamic range of 100 $\mu$T/10 fT = 200 dB, well beyond the capabilities of current electronics. In addition, the rotational speed must not cause the current flowing through the SQUID sensor to exceed its slew rate limitations. An ideal gradiometer is insensitive to a uniform field and would not suffer this dynamic range limitation.

## INPUT CIRCUITS

Whether an RF or dc SQUID, a SQUID system can be considered as a black box that acts like a current- (or flux-) to-voltage amplifier with extremely high gain. In addition, it offers extremely low noise, high dynamic range (>140 dB), excellent linearity ($>1:10^7$), and a wide bandwidth that can extend down to dc.

Today, SQUIDs are fabricated as planar devices. In this configuration, the superconducting loop, Josephson junctions and coils (input, feedback, and modulation) are patterned on the same device. Multilayer deposition techniques are used (primarily in LTS devices), and coils are normally in the form of a square washer. The planar configuration leads to quite small devices, occupying only a few cubic millimeters compared to 5+ cm$^3$ (1.2 cm diam. $\times$ 5 cm) for older toroidal RF SQUIDs (9). Another advantage of the planar device is that it is possible to have the detection coils as part of the SQUID sensor, eliminating the need for separate (three-dimensional) detection coils. Such an integrated sensor has the potential to reduce the complexity of multichannel systems significantly.

Although it is possible to couple magnetic flux directly into the SQUID loop, environmental noise considerations (see Fig. 9) make this difficult, if not impossible, in an unshielded environment. In addition, the area of a typical SQUID loop is small (<0.1 mm$^2$), and its resulting sensitivity to external flux changes ($\Delta\Phi = A \cdot \Delta B$) is also small. Although a larger loop diameter would increase the SQUIDs sensitivity to external flux, it would also make it much more susceptible to environmental noise. For this reason, external flux is normally inductively coupled to the SQUID loop by a flux transformer.

Conceptually, the easiest input circuit to consider for detecting changes in magnetic fields is that of a SQUID sensor connected to a simple superconducting coil (Fig. 5).

Because the total flux in a superconducting loop is conserved, any change in external field through the signal coil will induce a current in the flux transformer that must satisfy

$$\Delta\Phi = NA\Delta B = (L_{\text{coil}} + L_{\text{i}})\Delta I \tag{3}$$

where $\Delta B$ is the change in applied field; $N$, $A$, and $L_{\text{coil}}$ are the number of turns, area, and inductance of the detection coil; $L_{\text{i}}$ is the inductance of the SQUID input coil; and $\Delta I$ is the change in current in the superconducting circuit. If the lead inductance is not negligible, it must be added to $L_{\text{coil}}$ and $L_{\text{i}}$.

To calculate the sensitivity and noise level of a simple detection coil system, the inductance of the detection coil must be known. The inductance of a flat, tightly wound, circular multiturn loop of superconducting wire is given by (10)

$$4 \times 10^{-3} N^2 \pi r \left[\ln\left(\frac{8r}{\rho}\right) - 2\right] \quad \frac{\mu\text{H}}{\text{cm turn}^2} \tag{4}$$

where $r$ is the radius of the detection coil and $\rho$ is the radius of the (superconducting) wire. Knowing the coil inductance $L_{\text{coil}}$, we can rewrite Eq. (3) as

$$\Delta B = (L_{\text{coil}} + L_{\text{i}})\Delta I / NA \tag{5}$$

Because the SQUID system has an output proportional to the input current, maximum sensitivity is obtained by using the input circuit that provides the maximum current into the SQUID and satisfies all other constraints of the experimental apparatus. For a pure magnetometer, the maximum sensitivity will occur when the impedance of the detection coil matches that of the SQUID sensor ($L_{\text{coil}} = L_{\text{i}}$).

### Detection Coils

Several factors affect the design of the detection coils (11). These include the desired sensitivity of the system, the size and location of the magnetic field source, and the need to

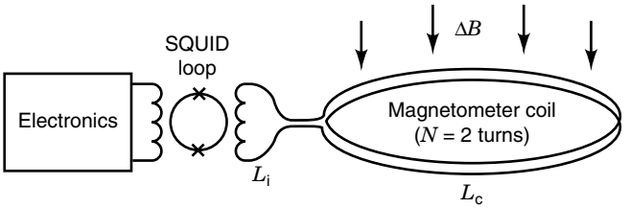


**Figure 5.** Schematic diagram of typical SQUID input circuit.

match the inductance of the detection coil to that of the SQUID. The ability to separate field patterns caused by sources at different locations and strengths requires a good signal-to-noise ratio. At the same time, one has to find the coil configuration that gives the best spatial resolution. Unfortunately, these two tasks are not independent. For example, increasing the signal coil diameter improves field sensitivity but sacrifices spatial resolution. In practice, system design is restricted by several constraints: the impedance and noise of the SQUID sensors, the size of the dewar, and the number of channels, along with the distribution and strength of noise sources.

It is extremely important for dc response that the detection coil(s) be superconducting. Resistance in the detection circuit has two effects: (1) attenuating the signal and (2) adding Nyquist noise. Resistive attenuation is important only below a frequency $f_0$, such that the resistive impedance is equal to the sum of the inductive impedances in the circuit (e.g., $f_0 \approx R/L_t$, where $L_t$ is the total inductive impedance of the circuit). Resistive noise is important only if it becomes comparable to other noise sources or the signal ($<10^{-30}$ J/Hz for biomagnetism, $<10^{-26}$ J/Hz for geophysics). For a SQUID with $E_N \approx 10^{-30}$ J/Hz, the total resistance of the circuit, *including any joints,* must be less than $1.4 \times 10^{-13}$ Ω (12). Thus it is very important that all solder joints, press-fits, or connections have as low a joint resistance as possible.

Figure 6 displays a variety of detection coils. The magnetometer [Fig. 6(a)] responds to the changes in the field penetrating the coil. More complicated coil configurations provide the advantage of discriminating against unwanted background fields from distant sources while retaining sensitivity to nearby sources.

Because of the present inability to make flexible wire or make true superconducting joints in HTS materials, three-dimensional HTS coil structures [e.g., Figs. 6(b,d–f)] are not possible. Present day HTS magnetometers are fabricated as planar devices and are available only as pure magnetometers [Fig. 6(a)] and planar gradiometers [Fig. 6(c)]. As a result, commercially available HTS devices are currently in the form of magnetic-sensing rather than current-sensing devices.

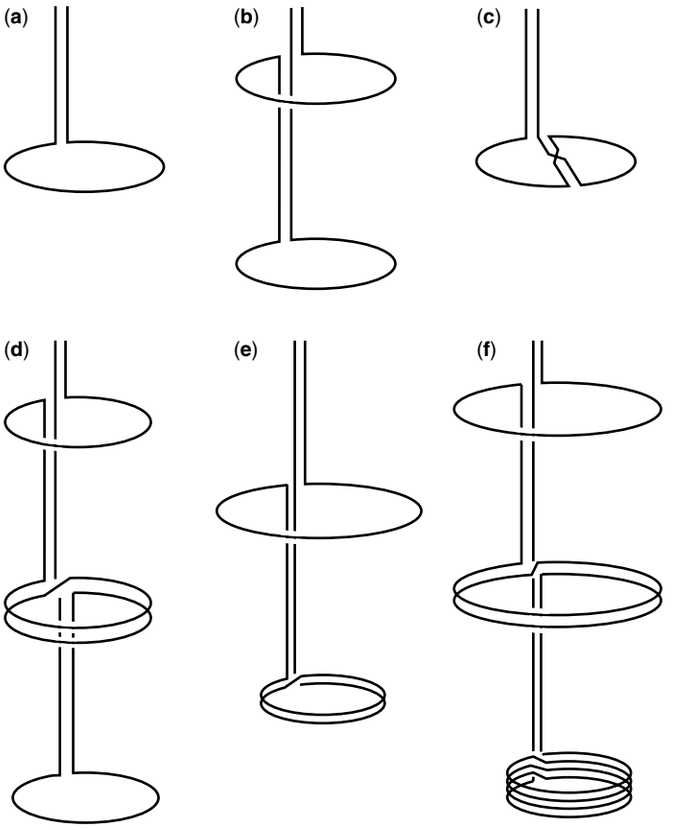


**Figure 6.** (a) magnetometer, (b) first derivative gradiometer, (c) planar gradiometer, (d) second derivative gradiometer, (e) first derivative asymmetric gradiometer, (f) second derivative asymmetric gradiometer. Courtesy of S. J. Williamson.

## Gradiometers

Magnetometers are extremely sensitive to the outside environment. This may be acceptable if one is measuring ambient fields. If what is to be measured is close to the detection coil and weak, outside interference may prevent measurements at SQUID sensitivities. If the measurement is of a magnetic source close to the detection coil, a gradiometer coil may be preferred. The field of a magnetic dipole is inversely proportional to the cube of the distance between the dipole and the sensor. It follows that the field from a distant source is relatively uniform in direction and magnitude at the sensor. If we connect in series two identical and exactly parallel loops wound in opposite senses, separated by a distance $b$ (the baseline), we obtain a coil [Fig. 6(b)] that will reject uniform fields.

Because the response of a single coil to a magnetic dipole goes as $1/r^3$, an object that is much closer to one coil than the other will couple better to the closer coil than the more distant. Sources that are relatively distant will couple equally into both coils. For objects that are closer than 0.3 $b$, the gradiometer acts as a pure magnetometer, while rejecting more than 99% of the influence of objects more than 300 $b$ distant (Fig. 7). In essence, the gradiometer acts as a compensated magnetometer. It is possible to use two gradiometers connected in series opposition [Fig. 6(d)] to further minimize the response of the system to distant sources. This can be extended to higher orders by connecting in series opposition two second-order gradiometers, etc. Doing so, however, reduces

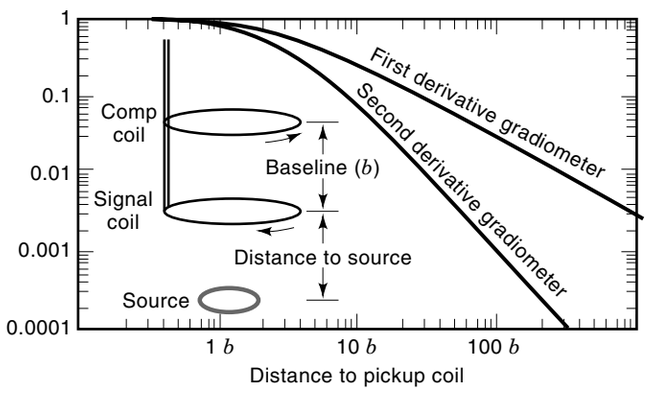


**Figure 7.** Response of gradient coils relative to magnetometer response ($1/r^3$ suppressed).

the sensitivity of the instrument to the signal of interest and may not significantly improve the signal-to-noise ratio.

Rejection of distant noise sources depends on having a precise match (or balance as it is sometimes referred to) between the number of area-turns in the coils. A symmetric gradiometer [Fig. 6(b) requires that $N_s A_s = N_c A_c$ where $N$ is the number of turns and $A$ is the area of the signal and compensation coils, respectively. An asymmetric design [Fig. 6(e,f)] has the advantage that the inductance ($L_s$) of the signal coil(s) is much greater than the compensation coils ($L_c$); greater sensitivity is achieved than with a symmetric design. Another advantage is that the signal coil diameter is reduced, leading to potentially higher spatial resolution. The optimum conditions for the number of turns in an asymmetric signal coil is given by (13):

$$(L_s + L_c + L_i + L_l) - N_s \frac{\partial}{\partial N_s}(L_s + L_c + L_i + L_l) = 0 \qquad (6)$$

If the gradiometer is perfectly made (balanced), it will reject uniform fields. However, if one coil has a larger effective diameter than the other, the response will not be that of a perfect gradiometer, but that of a gradiometer in series with a magnetometer. Mathematically, the balance, $\beta$ can be defined as $V_t \propto \boldsymbol{G} + \beta \cdot \boldsymbol{H}$, where $V_t$ is the system response, $\boldsymbol{G}$ is the coil's response to a gradient field, and $\boldsymbol{H}$ is the applied uniform fields. Typically, coil forms used to wind gradiometers can be machined (grooved) to achieve balances $\beta$ that range from 0.01 to 0.001. Planar devices, through photolithography, can achieve lower levels—a factor of 10 or better. Superconducting trim tabs placed within the detection coils can improve $\beta$ to the parts per million level. High degrees of balance can allow a SQUID gradiometer to operate in relatively large (millitesla) ambient fields while maintaining sensitivities in the tens of femtotesla.

For multichannel systems (such as are used in biomagnetism), it is not possible to use externally adjustable trim tabs—each tab tends to interfere with the others. The use of electronic balancing (14) can provide balance ratios at the parts per million level. In this situation, portions of (additional) magnetometer reference channel response are summed electronically with the gradiometers' input to balance out its effective magnetometer response. The use of eight-element tensor arrays as reference channels can further improve external noise rejection. The major advantage of electronic balancing is significant improvement in immunity to low-frequency environment noise.

## REFRIGERATION

The superconducting nature of SQUIDs require them to operate well below their superconducting transition temperature (9.3 K for Nb and 93 K for $YBa_2Cu_3O_{7-\delta}$). The thermal environment for the SQUID sensor and detection coil has typically been liquid helium or liquid nitrogen contained in a vacuum-insulated vessel known as a dewar (Fig. 8). The cryogen hold time depends on the boil-off rate (heat load) and the inner vessel volume.

The major heat load on dewars is the result of thermal conduction down the neck tube and a magnetometer probe along with black body radiation. The space between the inner and outer walls is evacuated to prevent thermal conduction between room temperature and the cryogen chamber. Within the vacuum space, a thermal shield (anchored to the neck tube) acts to reduce heat transfer by thermal (black body) radiation. The thermal shield either can be vapor cooled—using the enthalpy of the evaporating helium or nitrogen gas—or have the shield thermally connected to a liquid nitrogen reservoir. Dewars with remoable sections use liquid-nitrogen-cooled shields.

If the experiment involves measurements interior to the dewar, then a metallic dewar is preferable. Metallic dewars offer significant shielding from environmental noise at frequencies above 10 Hz to 100 Hz. If the system is to measure magnetic fields exterior to the dewar, the dewar must be magnetically transparent, and metallic construction is not appropriate. Dewars for external field measurements are normally constructed of nonmetallic, low-susceptibility materials to minimize their magnetic interactions with the SQUID sensors and detection coils. Materials used are typically glass-fiber epoxy composites such as G-10. In an effort to get the detection coil(s) as close as possible to the object being measured, a "tailed" design is often used. This decreases the forces on the bottom of the dewar and allows the use of thinner end pieces (closer tail spacing). Dewars for biomagnetic measurements often have curved tails to get closer to the head.

The major advantage of high-temperature superconductivity is the simplified cryogenics and reduced spacing between cryogenic regions and room temperature. The thermal load (due to conduction and black body radiation) is less, and the heat capacity of what needs to be cooled is larger (implying smaller temperature variations for a given heat load). Because the latent heat/unit volume of liquid nitrogen is 60 times larger than liquid helium, hold times become months rather than days for an equivalently sized dewar.

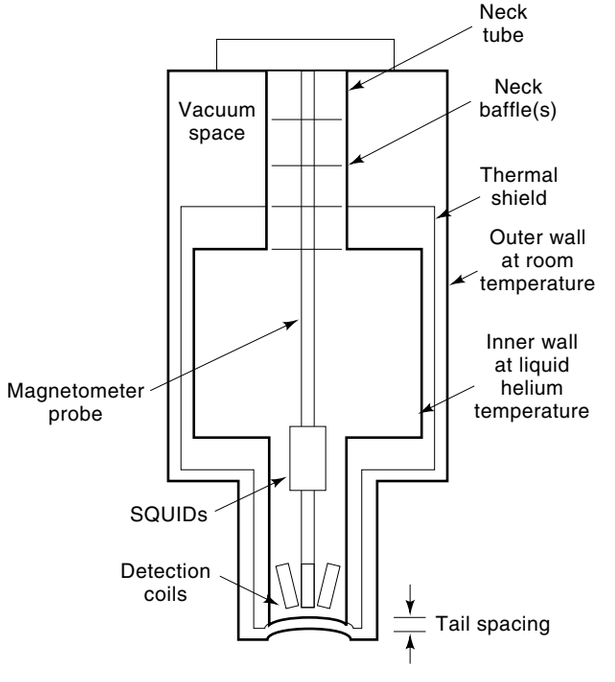


**Figure 8.** Typical design of a fiberglass dewar used for biomagnetic measurements.

### Closed Cycle Refrigeration

As an alternative to the use of liquid cryogens, closed cycle refrigeration would be desirable for several reasons. These include reduction of operating costs, use in remote locations, operation in nonvertical orientations, avoiding interruptions in cryogen deliveries, safety, and the convenience of not having to transfer every few days. Although one mechanically cooled SQUID system has been built (15), the inherent vibration and magnetic signature of present day closed cycle refrigerators prevent them from widespread use. The development of pulse tube refrigerators (16) offers promise for magnetometer operation without cryogens.

### Environmental Noise

The greatest obstacle to SQUID measurements is external noise sources. If the object being measured is within the cryostat (such as is typical in most laboratory experiments), metallic shielding can minimize external noise (e.g., act as a low-pass eddy current shield). Superconducting shields essentially eliminate all external field variations. This assumes that any electrical inputs to the experimental region have been appropriately filtered. Powerline or microprocessor clock frequencies can severely degrade performance.

When measuring external fields, the SQUID magnetometer must operate in an environment—the magnetic field of the earth—that can be ten orders of magnitude greater than its sensitivity (Fig. 9). The magnetic field at the surface of the earth is generated by a number of sources. There exists a background field of $\sim$50 $\mu$T with a daily variation of $\pm$0.1 $\mu$T. In addition, there is a contribution (below 1 Hz) from the interaction of the solar wind with the magnetosphere. The remaining contributions to external magnetic fields are primarily man-made. These can be caused by structural steel and other localized magnetic materials such as furniture and instruments that distort the earth's field and result in field gradients; moving vehicles that generate transient fields; electric motors; elevators; radio, television, and microwave transmitters; and the ever-present powerline electromagnetic field and its harmonics.

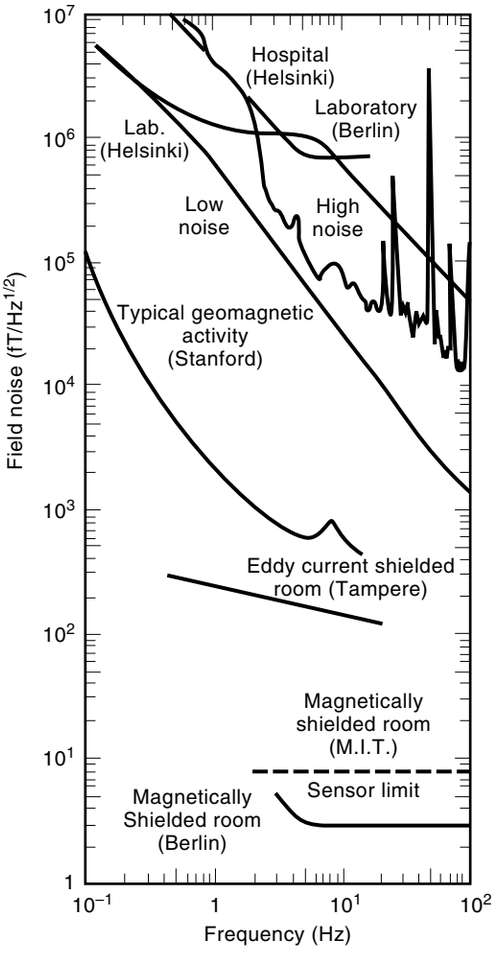


**Figure 9.** Rms field noise spectra in various environments as a function of frequency. Courtesy of S. J. Williamson.

### Noise Reduction

One method to attenuate external noise sources is with an eddy current shield that generates fields that act to cancel the externally applied fields within the conducting material. The shielding effect is determined by skin depth $\lambda$. For a sinusoidal varying wave

$$\lambda = \sqrt{\rho/\pi\mu_0 f} \tag{7}$$

where $f$ is the frequency of the applied field, $\rho$ is the electrical resistivity, and $\mu_0$ is the magnetic permeability of free space. In situations where the wall thickness $t \ll \lambda$, external fields are attenuated by

$$\frac{H_\mathrm{i}}{H_\mathrm{e}} = \frac{1}{1 + (2\pi f L/R)^2} \tag{8}$$

where $L$ is the inductance of the enclosure and $R$ is the resistance along the path of current flow. Unfortunately, induced currents in the shield generate noise. For a cylindrical shape,

$$B_\mathrm{rms} = \sqrt{\frac{64\pi k_\mathrm{B} T t}{h d \rho}} \tag{9}$$

where $h$ is the length and $d$ is the diameter of the can. The cut-off frequency is given by $f_{-3\,\mathrm{dB}} \approx \rho/4\pi dt$. Because of noise considerations, eddy current shields that are to be placed near the detection coils should be made from relatively poor conductors such as BeCu.

### Shielded Rooms

Another approach is to use eddy current shielding to shield the entire measurement system. An eddy current room constructed with 2 cm high purity aluminum walls can achieve shielding >40 dB at 60 Hz with improved performance at higher frequencies. The equivalent field noise is less than 200 fT/$\sqrt{\mathrm{Hz}}$ at frequencies above 1 Hz.

The need for shielding at lower frequencies has led to the use of magnetically shielded rooms (MSR). In the situation where $t \gg \lambda$, the attenuation goes as $(r/\lambda)e^{t/\lambda}$. Using pure eddy current shielding would require wall thicknesses that could exceed 1 m or more (below 1 Hz). For a ferromagnetic mate-

rial, the permeability of the material [$\mu = \mu_0(1 + \chi)$] replaces $\mu_0$ in Eq. (8). The shielding is due to the fact that flux prefers the path with the highest permeability. Because magnetically "soft" materials (e.g., mu-metal®) can have permeabilities that exceed $10^4$, the external magnetic flux is routed around the walls, avoiding the interior. The use of multiple shields can act to further shield the interior of a MSR. For the six-layer Berlin MSR (Fig. 9), shielding factors exceeded $10^4$ at frequencies above 0.01 Hz with noise levels below 3 fT/$\sqrt{\text{Hz}}$.

## APPLICATIONS

A large number of applications (Fig. 10) configure the SQUID as a magnetometer. SQUIDs can also be configured to measure a wide variety of electromagnetic properties (Fig. 11).

The state of the art in materials processing limits the variety of superconducting input circuits that can be used with HTS SQUIDs. As already mentioned, there is no existing method for making superconducting connections to SQUIDs with HTS wire. As a result, commercially available HTS devices are currently in the form of magnetic sensing [Fig. 6(b)] rather than current sensing devices [Fig. 6(a,c–f)].

### Laboratory Applications (4,8,17)

Table 1 shows typical capabilities of commercially available SQUID-based instruments. The number in the parenthesis refers to the corresponding Fig. 11.

**Current.** One common use of a SQUID is as an ammeter [Fig. 11(a)]. The input can be connected to an experiment at liquid helium temperatures or to room temperature. If the signal is to be inductively coupled to a detection coil that is connected to the SQUID input, then the circuit must be superconducting if dc response is desired.

If the measurement is of a current that passes through the detection coil, a toroidal geometry for the detection coil has the advantage of extremely good coupling to the source while rejecting contributions due to external sources. Because the measurement is inductive, there is no loading of the current-generating elements.

**Voltage.** Typically the majority of applications use superconducting circuits. There are, however, a number of applications where resistive circuits are used. One example is the detection of extremely small voltages or resistances (Fig. 12).

When a voltage $V_I$ is applied across the input terminals, a current is generated in the SQUID input coil. In this situation, the feedback current ($I_F$) that would normally be applied to the SQUID loop is fed back via $R_F$ through $r_s$ until the voltage drop across $r_s$ is equal to $V_I$ and there is no net current through the SQUID. $V_O$ measures the voltage drop across $R_F$ and $r_s$ with $V_I = V_O r_s/(R_F + r_s)$. The voltage gain of the system is determined by the ratio of $R_F/r_s$. Typical values for $R_F$ and $r_s$ are 3 and 30 $\mu\Omega$, respectively, giving a voltage gain of $10^8$. The standard resistor $r_s$ is typically at 4.2 K. The voltage source, however, may be at a completely different temperature.

The input noise of a SQUID picovoltmeter ($\sim 10^{-14}$ V) is a function of the source resistance and temperature ($R \propto T_s$), the inherent voltage noise (due to $\boldsymbol{r}_s$), and the inherent current noise of the SQUID. Measurement of the Johnson noise in a resistor ($\langle V^2 \rangle = 4\, k_B T R\, \Delta f$ where $\Delta f$ is the bandwidth of the measurement) can be used to determine absolute temperature. Commercially available LTS SQUIDs have equivalent device temperatures $<1$ $\mu$K and are suitable for noise thermometry.

With the addition of an appropriate current source [Fig. 11(d)], it is possible to measure resistance. Resolutions of $10^{-11}$ $\Omega$ can be achieved for $R_x < 10^{-2}$ $\Omega$. Other applications of picovoltmeters include measurements of thermopower, thermal electromotive forces (emfs) (thermocouples), and infrared bolometers.

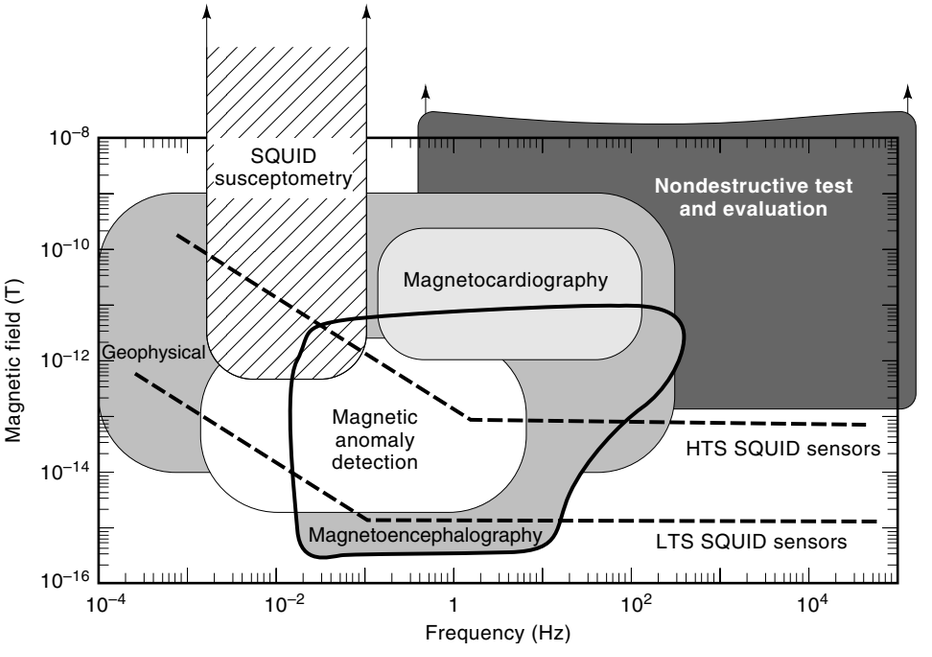


**Figure 10.** Field sensitivities and bandwidths typical of various applications. The lines indicate the sensitivity of commercially available SQUIDs.

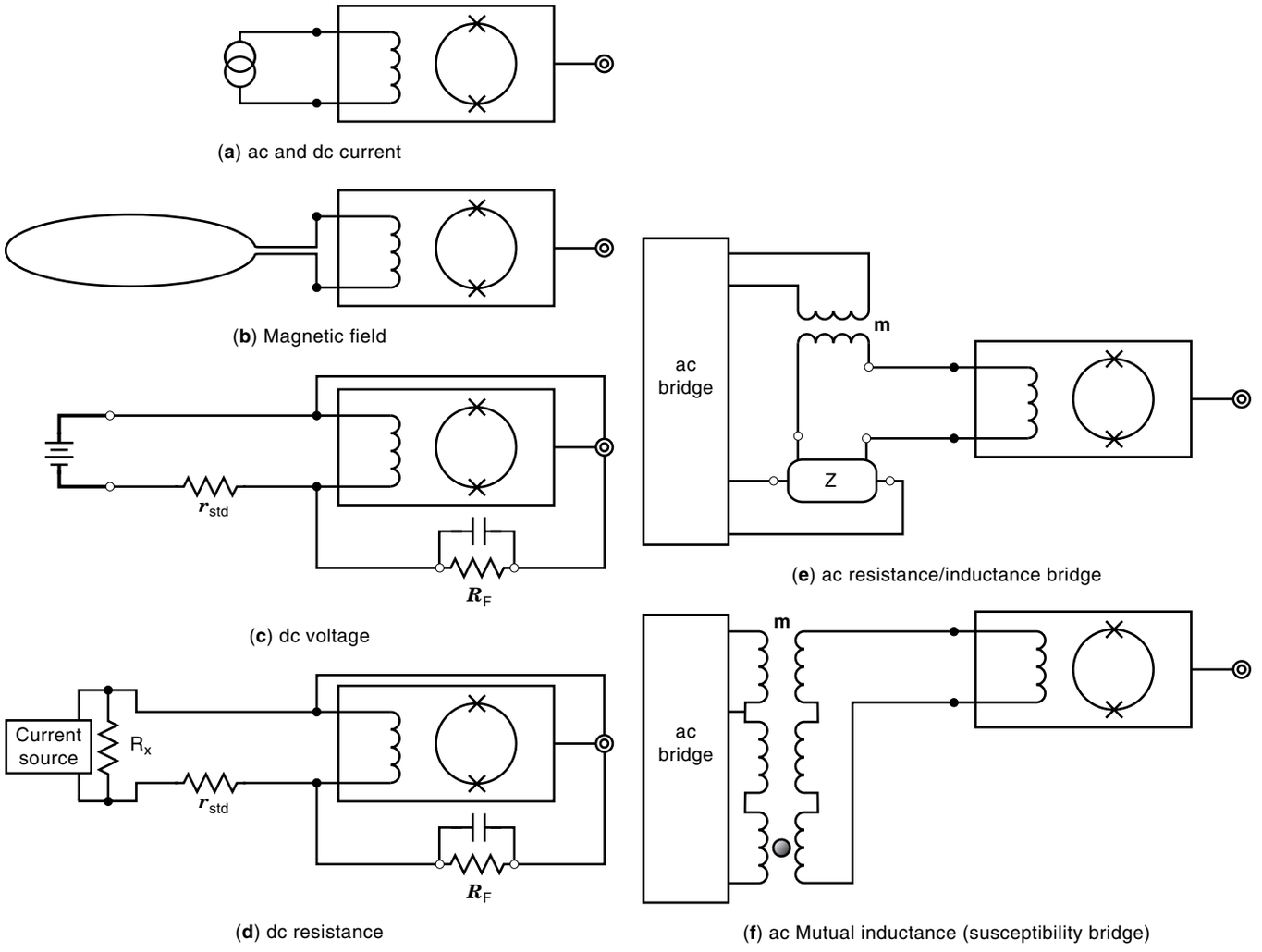


**Figure 11.** (a) ac and dc current, (b) magnetic field, (c) dc voltage, (d) dc resistance, (e) ac resistance/inductance bridge, (f) ac mutual inductance (susceptibility bridge).

**Ac Susceptibility (4).** The SQUID can also be used as the null detector in an ac bridge circuit (Fig. 13) to measure both resistive and reactive components of a complex impedance. The unknown impedance **Z** is excited by a current generated by an oscillator voltage, which is attenuated by a precision ratio transformer $\lambda$. The difference between the voltage developed across the unknown impedance **Z** and that developed in the secondary of a nulling mutual inductor **m** is applied to the input of the SQUID circuit. The primary current in **m** is proportional to the oscillator voltage and defined by the set-

**Table 1. Typical Capabilities of SQUID-based Instruments**

| Measurement | Sensitivity |
|---|---|
| Current [Fig. 11(a)] | $10^{-12}$ A/$\sqrt{\text{Hz}}$ |
| Magnetic fields [Fig. 11(b)] | $10^{-15}$ T/$\sqrt{\text{Hz}}$ |
| dc voltage [Fig. 11(c)] | $10^{-14}$ V |
| dc resistance [Fig. 11(d)] | $10^{-12}$ Ω |
| Mutual/self inductance [Fig. 11(e)] | $10^{-12}$ H |
| Magnetic moment [Fig. 11(f)] | $10^{-10}$ emu |

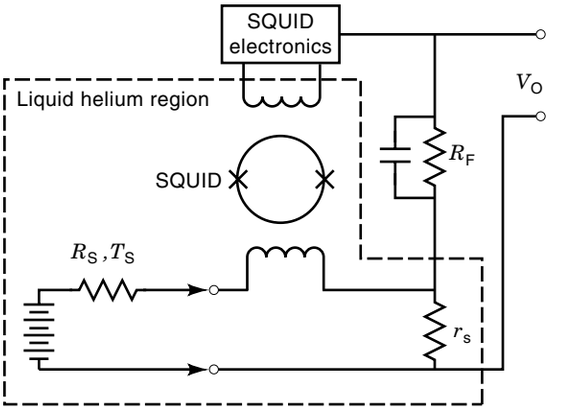


**Figure 12.** Block diagram of SQUID picovolt measuring system. Negative feedback is applied to the cryogenic input circuit through the voltage divider formed by $R_F$ and $r_s$.

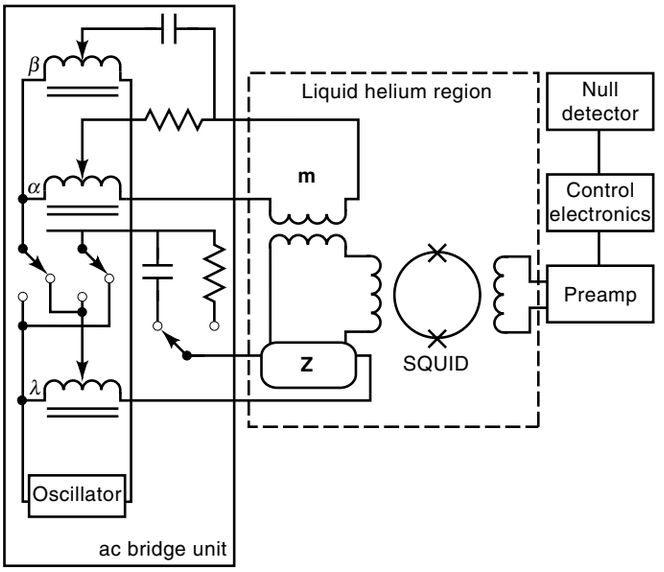


**Figure 13.** Block diagram of ac bridge.

ting of the ratio transformer $\alpha$. An additional reactive current is supplied by a second ratio transformer $\beta$, which causes the primary current to be passed through a capacitor rather than a resistor, thus generating a 90° phase shift in the voltage applied to **m**. The amplified off-balance signal, which appears at the output of the SQUID control electronics, can be displayed by means of a lock-in amplifier tuned to the oscillator frequency.

As mentioned earlier, the sensitivity is limited inherently by Johnson noise in the resistive components of the unknown (including the potential connections) and by the device noise of the SQUID sensor. Assuming $I_N \approx 1$ pA/$\sqrt{\text{Hz}}$, such a system is capable of measuring $R$ between $10^{-10}$ to 0.5 Ω and $L$ (self and mutual) between $10^{-12}$ and $10^{-3}$ H. Using a current comparator as the bridge excitation **V**, a 0.1 ppm resistance bridge can be constructed.

**SQUID Magnetometer/Susceptometers (16).** Instead of using a secondary ac excitation coil [Fig. 11(f)], a dc field can be used to magnetize samples. Typically the field is fixed, and the sample is moved into the detection coil's region of sensitivity. The change in detected magnetization is directly proportional to the magnetic moment of the sample. Because of the superconducting nature of SQUID input circuits, true dc response is possible.

Commonly referred to as SQUID magnetometers, these systems are properly SQUID susceptometers. They have a homogeneous superconducting magnet to create a very uniform field over the entire sample measuring region and the superconducting pick-up loops. The magnet induces a moment allowing a measurement of magnetic susceptibility. The superconducting detection loop array is rigidly mounted in the center of the magnet (17). This array is configured as a gradient coil to reject external noise sources. The detection coil geometry determines what mathematical algorithm is used to calculate the net magnetization. Oppositely paired Helmholtz, first and second derivatives have all been successfully used. Coupling two axial channels of differing gradient order can significantly improve noise rejection.

Sensitivities of $10^{-8}$ emu have been achieved, even at applied fields of 9 T. Placement of secondary excitation coils can allow ac susceptibility measurements to be made in the presence of a significant dc bias field. Variable temperature capability (1.7 K to 800 K) is achieved by placing a reentrant cryostat within the detection coils.

**Other Laboratory Applications.** NMR signals (18) can be measured by placing a sample (e.g., protons or $^{19}$F) in the center of SQUID detection coils and either sweeping the external field or appying an rf excitation to the sample. The same experimental concept can be used to measure electron paramagnetic resonance (EPR) signals. SQUIDs have been used for more esoteric applications including temperature measurements with resolution near 10 K to 12 K. SQUIDs have also been used to measure position for gravity wave detectors with sub Ångstrom resolution and tests of Einstein's General Theory of Relativity. Because SQUID magnetometers are vector devices, they can detect rotations better than $10^{-3}$ arc-seconds in the earth's magnetic field. SQUIDs have been used in searches for dark matter such as Weak Interacting Massive Particles (WIMPs) along with attempts at detecting magnetic monopoles and free quarks.

## Geophysical Applications (19,20)

SQUID magnetometers are used to measure the earth's magnetic field (Fig. 9) at frequencies ranging between 1 kHz and $10^{-4}$ Hz. A technique known as magnetotellurics (21) can be used to determine the electrical conductivity distribution of the earth's crust by measuring the earth's electric and magnetic field. Because the earth is a good electrical conductor compared to the air, the electrical field generated in the ionosphere (as a result of solar wind) is reflected at the earth's surface, with components of both the electric and magnetic field decaying as they penetrate into the earth. The decay length or skin depth $\delta = 500\sqrt{\rho\tau}$, where $\rho$ is the electrical resistivity of the earth and $\tau$ is the period of the electromagnetic wave.

In magnetotellurics, the electric field (as a function of frequency) is related to the magnetic field via an impedance tensor where $\mathbf{E}(\omega) = \mathbb{Z}\ \mathbf{H}(\omega)$. The impedance tensor $\mathbb{Z}$ contains four complex elements $Z_{xx}$, $Z_{xy}$, $Z_{yx}$, and $Z_{yy}$ and is related to the resistivity by $\rho ij = 0.2\ |Z_{ij}(\omega)|^2\tau$ where $\mathbb{Z}$ has units of mV/km-nT.

Magnetic anomaly detection uses the five unique spatial components of $\nabla\mathbf{B}$ to locate a magnetic dipole uniquely. This has potential uses in mineralogical surveys and detection of unexploded ordnance.

## Nondestructive Test and Evaluation (22,23)

Magnetic-sensing techniques such as eddy current testing have been used for many years to detect flaws in structures. A major limitation on their sensitivity is the skin depth [Eq. (7)] of metallic materials. Because SQUID sensors have true dc response and superior sensitivity, they can see "deeper" into metallic structures. dc response also means that they can detect remnant magnetization—without the need for externally applied magnetic fields. Their flat frequency response and zero phase distortion allows for a wide range of applica-

**Table 2. NDE Measurement Techniques**

| |
|---|
| Imaging |
| Intrinsic currents |
| Remnant magnetization |
| Flaw-induced perturbations in applied currents |
| Johnson noise in metals |
| Eddy currents in an applied ac field (flaws) |
| Embedded magnetic sensors |
| Hysteretic magnetization due to: |
| Cyclic stress (strain) |
| Simultaneous dc & ac magnetic fields |
| Magnetization of paramagnetic, diamagnetic and ferromagnetic materials in dc magnetic fields |

**Table 3. Medical Applications of SQUIDs**

| |
|---|
| Studies of the brain—neuromagnetism |
| Epilepsy |
| Presurgical cortical function mapping |
| Drug development and testing |
| Stroke |
| Alzheimer's |
| Neuromuscular disorders |
| Prenatal brain disorders |
| Performance evaluation |
| Studies of the heart—magnetocardiography |
| Arrhythmia |
| Heart muscle damage |
| Fetal cardiography |
| Other medical applications |
| Studies of the stomach—gastroenterology |
| Intestinal ischemia |
| Noninvasive in vivo magnetic liver biopsies |
| Lung function and clearance studies |
| Nerve damage assessment |

tions. One potential application of SQUIDs is in detection of stress or corrosion in reinforcing rods used in bridges, aircraft runways, or buildings. Table 2 shows some of the measurement techniques that can be used with SQUID sensors.

SQUID magnetometers have been used to make noncontact measurements of timing circuits (24)—one instrument has better than 10 $\mu$m resolution (25). Such instruments with MHz bandwidths could be used for circuit board and integrated circuit (IC) mapping.

### Medical Applications of SQUIDs (23,26–29)

The use of bioelectric signals as a diagnostic tool is well known in medicine [e.g., the electrocardiogram (ECG) for the heart and the electroencephalogram (EEG) for the brain]. The electrical activity that produces the surface electrical activity that is measured by EEG and ECG also produces magnetic fields. The analogous magnetic measurements are known as the magnetocardiogram (MCG) and the magnetoencephalogram (MEG). Other physiological processes also generate electrical activity with analogous magnetic fields (Fig. 14).

Magnetic fields from active electrical sources in the body can be measured passively and external to the body by placing the magnetometer in close proximity to the body's surface. It has been shown that a population of neurons in the brain can be modeled as a current dipole that generates a well-defined magnetic field profile. Mapping of these field profiles can be used to infer the location of the equivalent active dipole site region to within millimeters. Using evoked response techniques, the location of signal pathways and information processing centers in the brain can be mapped at different delay times (latencies) following the stimulus.

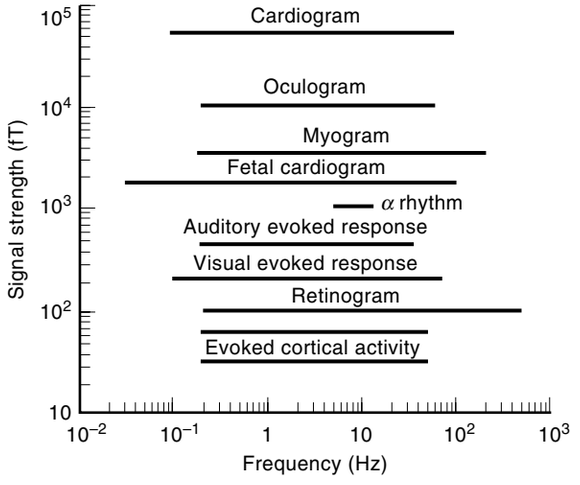


**Figure 14.** Typical amplitudes and frequency ranges for various biomagnetic signals.

There are also magnetic mesurements for which there are no electrical analogs. These are measurements of static magnetic fields produced by ferromagnetic materials ingested into the body and measurements of the magnetic susceptibility of materials in the body. In particular, information on the quantity and depth of diamagnetic or paramagnetic materials (such as iron stored in the liver) can be obtained by using magnetizing and detection coils of differing sizes in the same instrument and measuring the induced field as a function of distance. This technique is already being used to monitor patients suffering from iron overload diseases such as thalassemia and hemochromatosis.

The development of the SQUID has allowed the development of noninvasive clinical measurements of biomagnetic fields. The use of gradiometers can allow measurements to be made in unshielded environments at sensitivities below 20 fT/$\sqrt{\text{Hz}}$. Typically, however, neuromagnetic measurements are made in room-sized MSRs that will allow measurements of the magnetic field of the brain over the entire surface of the head (>150 positions simultaneously). Table 3 gives some of the areas in which SQUID magnetometers are currently being used in medical research.

## BIBLIOGRAPHY

1. B. D. Josephson, Possible new effect in superconductive tunneling, *Phys. Lett.,* **1**: 251–253, 1962.
2. J. Clarke, SQUID fundamentals, in H. Weinstock (ed.), *SQUID Sensors: Fundamentals, Fabrications and Applications,* Dordecht: Kluwer, 1997.
3. T. Van Duzer and C. W. Turner, *Principles of Superconductive Devices and Circuits,* New York: Elsevier, 1981.
4. T. P. Orlando and K. A. Delin, *Foundations of Applied Superconductivity,* Reading, MA: Addison-Wesley, 1991.

5. R. P. Giffard, R. A. Webb, and J. C. Wheatley, Principles and methods of low-frequency electric and magnetic measurements using an rf-biased point-contact superconducting device, *J. Low Temp. Phys.,* **6**: 533–610, 1972.
6. R. J. Prance et al., Fully engineered high performance UHF SQUID magnetometer, *Cryogenics,* **21**: 501–506, 1981.
7. C. D. Tesche and J. Clarke, DC SQUID: noise and optimization, *J. Low Temp. Phys.,* **29**: 301–331, 1982.
8. M. B. Simmonds and R. P. Giffard, *Apparatus for reducing low frequency noise in dc biased SQUIDs,* US Patent No. 4,389,612, 1983.
9. R. L. Fagaly, Superconducting magnetometers and instrumentation, *Sci. Prog., Oxford,* **71**: 181–201, 1987.
10. F. W. Grover, *Inductance Calculations, Working Formulas and Tables,* New York: Dover, 1962.
11. J. P. Wikswo, Jr., Optimization of SQUID differential magnetometers, *AIP Conference Proc.,* **44**: 145–149, 1978.
12. R. B. Stephens and R. L. Fagaly, High temperature superconductors for SQUID detection coils, *Cryogenics,* **31**: 988–992, 1991.
13. R. Illmoniemi et al., Multi-SQUID devices and their applications, in D. F. Brewer (ed.), *Progress in Low Temperature Physics,* vol. XII, Amsterdam: Elsevier, 1989.
14. J. Vrba, SQUID gradiometers in real environments, in H. Weinstock (ed.), *SQUID Sensors: Fundamentals, Fabrications and Applications,* Dordecht: Kluwer, 1997.
15. D. S. Buchanan, D. N. Paulson, and S. J. Williamson, Instrumentation for clinical applications of neuromagnetism, in R. W. Fast (ed.), *Advances in Cryogenic Engineering,* vol. 33, New York: Plenum, 1988, pp. 97–106.
16. C. Heiden, Pulse tube refrigerators: A cooling option, in H. Weinstock (ed.), *SQUID Sensors: Fundamentals, Fabrications and Applications,* Dordecht: Kluwer, 1997.
17. R. E. Sarwinski, Superconducting instrumentation, *Cryogenics,* **17**: 671–679, 1977.
18. R. A. Webb, New technique of improved low-temperature SQUID NMR measurements, *Rev. Sci. Instrum.,* **48**: 1585, 1977.
19. J. Clarke, Geophysical Applications of SQUIDs, *IEEE Trans. Mag.,* **MAG-19**: 288–294, 1983.
20. H. Weinstock and W. C. Overton, Jr. (eds.), *SQUID Applications to Geophysics,* Tulsa: Soc. of Exploration Geophysicists, 1981.
21. K. Vozoff, The magnetotelluric method in the exploration of sedimentary basins, *Geophysics,* **37**: 98–114, 1972.
22. G. B. Donaldson, SQUIDs for everything else, in H. Weinstock and M. Nisenoff (eds.), *Superconducting Electronics,* New York: Springer-Verlag, 1989.
23. J. P. Wikswo, Jr., SQUID magnetometers for biomagnetism and non-destructive testing: Important questions and initial answers, *IEEE Trans. Appl. Supercond.,* **5**: 74–120, 1995.
24. R. L. Fagaly, SQUID detection of electronic circuits, *IEEE Trans. Magn.,* **MAG-25**: 1216–1218, 1989.
25. J. Kirtley, Imaging magnetic fields, *IEEE Spectrum,* **33** (12): 40–48, 1996.
26. S. J. Williamson and L. Kaufman, Biomagnetism, *J. Magn. Mag. Mat.,* **22**: 129–202, 1981.
27. G-L. Romani, S. J. Williamson, and L. Kaufman, Biomagnetic instrumentation, *Rev. Sci. Instrum.,* **53**: 1815–1845, 1982.
28. R. L. Fagaly, Neuromagnetic instrumentation, in S. Sato (ed.), *Advances in Neurology, Vol. 54: Magnetoencephalography,* New York: Raven Press, 1990.
29. C. Aine et al., *Advances in Biomagnetism Research: Biomag96,* New York: Springer-Verlag, 1997.

ROBERT L. FAGALY
Tristan Technologies